Original Article

Polydopamine coating promotes early osteogenesis in 3D printing porous Ti6Al4V scaffolds

Lan Li[1,2,3#], Yixuan Li[2#], Longfei Yang[1], Fei Yu[4], Kaijia Zhang[2], Jing Jin[2], Jianping Shi[5], Liya Zhu[5], Huixin Liang[6], Xingsong Wang[1], Qing Jiang[2,3]

[1]School of Mechanical Engineering, Southeast University, Nanjing 210000, China; [2]Department of Sports Medicine and Adult Reconstructive Surgery, Drum Tower Hospital affiliated to Medical School of Nanjing University, Nanjing 210000, China; [3]Institute of Medical 3D Printing, Nanjing University, Nanjing 210000, China; [4]Drum Tower of Clinical Medicine, Nanjing Medical University, Nanjing 210000, China; [5]School of Electrical and Automation Engineering, Nanjing Normal University, Nanjing 210000, China; [6]School of Mechanical and Electrical Engineering, Nanjing University of Aeronautics and Astronautics, Nanjing 210000, China

Contributions: (I) Conception and design: L Li, Y Li, Q Jiang; (II) Administrative support: X Wang, Q Jiang; (III) Provision of study materials or patients: L Zhu; (IV) Collection and assembly of data: H Liang; (V) Data analysis and interpretation: L Yang, K Zhang, F Yu, L Zhu, J Shi, H Liang; (VI) Manuscript writing: All authors; (VII) Final approval of manuscript: All authors.

[#]These authors contributed equally to this work.

Correspondence to: Xingsong Wang, PhD. School of Mechanical Engineering, Southeast University, No. 2 Southeast University Road, Nanjing 210000, China. Email: xswang@seu.edu.cn; Qing Jiang, MD, PhD. Department of Sports Medicine and Adult Reconstructive Surgery, Drum Tower Hospital Affiliated to Medical School of Nanjing University, Nanjing 210000, China. Email: qingj@nju.edu.cn.

Background: Titanium implants are widely used in orthopedic and dental for more than 30 years. Its stable physicochemical properties and mechanical strength are indeed appropriate for implantation. However, the Bioinertia oxidized layer and higher elastic modulus often lead to the early implantation failure.

Methods: In this study, we proposed a simple design of porous structure to minimize the disparity between scaffold and natural bone tissue, and introduced a one-step reaction to form a polydopamine (PDA) layer on the surface of titanium for the purpose of improving osteogenesis as well. The porous scaffolds with pore size of 400 μm and porosity of 44.66% were made by additive manufacturing. The cell behavior was tested by seeding MC3T3-E1 cells on Ti6Al4V films for 15 days. The biomechanical properties were then analyzed by finite element (FE) method and the *in vivo* osteogenesis effect was accordingly evaluated by implanting the scaffolds for 5 weeks in rabbits.

Results: According to the achieved results, it was revealed that the immersion for 40 min with dopamine could significantly improve the cell adhesion. The proposed method for design of porous structure can avoid the stress shielding effect and bone growth inside the PDA coating scaffolds, which were observed at the early stage of bone healing process.

Conclusions: It can be concluded that the proposed PDA coating method is effective in promoting early osteogenesis, as well as being easy to operate, and can be helpful in the future clinical application of titanium implants.

Keywords: 3D printing; Ti6Al4V scaffold; polydopamine (PDA); surface modification; finite element simulation (FE simulation)

Submitted Jan 17, 2019. Accepted for publication Apr 17, 2019.
doi: 10.21037/atm.2019.04.79
View this article at: http://dx.doi.org/10.21037/atm.2019.04.79

Introduction

In tissue engineering, scaffolds are momentous in supporting cell attachment, proliferation, and differentiation. For bone tissue engineering, load-bearing and bong-contacting are necessary for scaffolds to provide the osteoconductive and osteoinductive characteristics for bone remodeling, as well as bone ingrowth during the fracture healing process, prosthesis osseointegration, and distraction osteogenesis (1). Mechanical function and high-level of mechanical stresses can be restored with ideal scaffolds (2). Titanium and its alloys with excellent mechanical properties, satisfactory biocompatibility, and chemical stability are regarded as appropriate implant materials in orthopedic and dental applications (3,4). For more than 30 years, artificial bones and joints, plates, and screws made by titanium alloys have been widely used in clinics as orthopedic implants and substitute materials for hard tissues (5-7), however, there are currently some difficulties and limitations that should be solved. Compared with other metallic materials, the elastics modulus of titanium alloys is closer to that of cortical bones and cancellous bones, however, the disparity between these kinds of materials are reported at the range of 7 to 10 times (8,9). This huge modulus mismatch plays a vital role influencing stress shielding, which may cause osteoporosis and fracture around the implants (10). The porous designs have been employed to overcome this problem and mimic the elasticity modulus and yield strength of natural bone (11,12). The interconnected pores with pore size ranging from 100 to 500 μm have been proved appropriate for exchanging nutrients, vascularization, and bone ingrowth (13,14). Several *in vivo* studies on rodents have demonstrated that the porous structure can improve the interfacial bond between the implant surface and the surrounding tissue, promote the vascularization and bone ingrowth, and provide mechanical stability at early stage after being embedded (11,15,16). However, the fine and stable physicochemical properties make titanium alloys difficult to machining, especially for fabricating porous structures. Traditional fabrication processes, such as powder sintering, plasma spray coating, fiber bonding, and phase separation, are difficult to control the pore characteristics, including pore size, pore shape, and pore size distribution (17,18).

In the present study, we proposed the selective laser melting (SLM), a kind of three-dimensional (3D) printing technology, to fabricate the porous titanium scaffolds. The Ti6Al4V powder can completely melt under the high-energy density laser and form 3D entities after cooling. Compared with selective laser sintering (SLS), this rapid technique can avoid the non-design micro pores and improve the mechanical strength of the printing entities. The nanolaser beam with diameter of 30 μm with layer thickness of 50 μm can build up porous structures in any complexity to reduce the weight and keep enormous strength for the purpose of bone tissue repairing (19). The internal and external shape of 3D printing product made by SLM can be closer to the computer aided design (CAD) model, ensure that the scaffold pore characteristics can fix the requirements of bone formation. Fine and precisely controlled porous structures with pore size ranging from 300 to 700 μm can be produced by SLM technology (11,20). The unique and mechanically strong osteoconductive scaffolds made by this technology are suitable for repairing cortical bone defects due to the fully interconnected structures. Several researchers have employed this method to fabricate porous scaffolds for bone tissue engineering in rats model and rabbit model (21-23).

Except for the mechanical properties, the key point to successful implantation is the long-term osseointegration of the scaffolds and bone surface (24). Although the structural design can partially solve the issues in biomechanics, the porous titanium requires sufficient ability in inducing osseointegration of surface to promote bone growth into the inner pores of scaffolds. Unfortunately, the inherent Bioinertia of titanium cannot meet the requirement to achieve the early osseointegration (25). The biological inertia proved to be double-edged for titanium implants. On the one hand, the layer of dense titanium dioxide (TiO_2) film develops on the surface of titanium alloys, providing strong corrosion resistance and stable biochemistry properties, and causes titanium to be attractive for application in hard tissues. On the other hand, this Bioinertia oxidized layer hinders the direct interaction between the implant and bone tissue, leading to the implantation failure (26,27). To address this issue, surface modifications with some bioactive substances, such as calcium (Ca), zinc (Zn), graphene, bone morphogenetic protein-2 (BMP-2), and Arg-Gly-Asp (RGD) peptides, have been applied to improve the biological performance of porous titanium scaffolds (24,28-30). The physical adsorption on titanium alloys introduced by electrostatic interactions are simplicity, flexibility, but instability. The reversible interactions can be easily reversed post implantation (31,32). The chemical conjugation between substrate surfaces and grafting molecules is the key factor for stable covalent modifications (33). The traditional covalent modification methods for titanium surfaces contain

disadvantages such as, complex chemical reaction as well as being time-consuming process (34,35). However, the underwater adhesive proteins containing 3,4-dihydroxy-L-phenylalanine (DOPA) from mussel protein have demonstrated universal applicability to form strong adhesive interaction with various material surfaces, including polymers, metals, and ceramics (36-39). The catechol groups of dopamine can simply form a polydopamine (PDA) layer on the surfaces of titanium in an alkaline environment, and it plays vital roles in adhesion and surface modification (40). In addition, the PDA coating is one of the most advantageous features among its extensive chemical properties associated with bone regeneration by improving the interfacial properties of implants (41). According to a number of previous studies, the PDA coating can stimulate initial cell adhesion and proliferation, and increase the expression of bone-related genes (42,43). Additionally, the PDA can integrate inorganic hydroxyapatite (HA) crystals on surface of titanium and bioceramics via a simple reaction in a simulated body fluid (42-44).

According to the above-mentioned statements, the present study aimed to explore the early bone formation ability of Ti6Al4V porous scaffolds coating by PDA. For reducing the effect of structural design on bone formation, we proposed a simple porous structure with pore size of 400 μm and porosity of 44.66%. To observe the cell behavior affected by PDA coating, the mouse pre-osteoblast cell line MC3T3-E1 were seeded on the Ti6Al4V films for as long as 15 days. The finite element (FE) simulation was then used to analyze the stress of the implants and the surrounding bone tissue. Eventually, an *in vivo* study on rabbits was conducted to evaluate the effect of bone formation at early stage of bone healing process.

Methods

The experiment was divided into three parts: *in vitro* test, FE simulation, and *in vivo* test. All methods in this study were carried out in accordance with relevant guidelines and regulations. All experimental protocols in this study were approved by the ethics committee of Drum Tower Hospital affiliated to Medical School of Nanjing University.

In vitro test

Substrate preparation and PDA coating

Ti6Al4V films with diameter of 14 mm and thickness of 1 mm were ultrasonically cleaned three times in acetone, ethanol, and deionized water (dH_2O) before use. For the PDA coating, the films were immersed into a dopamine solution (2 mg/mL, 10 mM Tris-HCl buffer, pH =8.5; Sigma-Aldrich, MO, USA) at room temperature (43). The coating process was carried out for 40 min. The PDA-coated films were then ultrasonically rinsed with dH_2O three times to remove the unattached dopamine molecules and dried with nitrogen gas. The PDA coating was characterized by a scanning electron microscope (SEM; Hitachi Ltd., Tokyo, Japan) and an energy dispersive spectrometer (EDS; Hitachi Ltd., Tokyo, Japan).

Cell culture

Mouse pre-osteoblast cell line MC3T3-E1 (Subclone 4) were obtained from Nanjing University and cultured in a humidified incubator with 95% air and 5% CO_2. They were maintained in minimum essential medium α (α-MEM; Gibco, USA) with 10% fetal bovine serum (FBS; Gibco, USA) and plated with a cell density of 20,000 cells/cm^2 onto the PDA-coated films in a 24-well cell culture plate. The cells were then cultured at 37 ℃ for 1, 3, 5, 7, and 15 days. Cells cultured on the unmodified Ti films were set as control groups.

Assessment of cell viability

Cell compatibility assays were performed using Cell Counting Kit-8 (Sigma-Aldrich, MO, USA). MC3T3-E1 cells were cultured on unmodified Ti films and PDA-coated Ti films. After each time point, mixture of 50 μL CCK-8 reagent with 450 μL culture medium was added to each well plate and incubated for another 2 h at 37 °C. Then, 100 μL suspensions were extracted to a 96-well plate, and the absorbance at 450 nm was determined using a microplate reader.

The films were sputter-coated with platinum and then observed under SEM. The cell-films were washed with phosphate buffered saline (PBS), fixed with 3% glutaraldehyde at 4 ℃ overnight, and treated with the 1% osmium tetroxide for 1 h. After that, the films were dehydrated using ethanol solution (50, 75, 95, and 100 wt%), freeze-dried, and observed by SEM.

Immunofluorescence staining

Supernatants were removed and Ti substrates with MC3T3-E1 cells were washed with PBS twice. Then, those were fixed with 4% paraformaldehyde (Sigma-Aldrich, MO, USA) for 20 min and permeabilized with 0.1% Triton X-100 (Sigma-Aldrich, MO, USA) for 5 min, which followed by incubation with 2% bovine serum albumin (BSA) blocking

Table 1 The properties of materials used in FE simulation

Materials	Density (kg/m^3)	Young's modulus (GPa)	Yield modulus (MPa)	Poisson's ratio
Ti6Al4V	4,430	105	830	0.31
Bone	1,700	7.8	85	0.3

FE, finite element.

buffer for 30 min. The cells were stained with FITC-phalloidin (1:200; Sigma-Aldrich, MO, USA) at 37 ℃ for 60 min in the dark. After washing with PBS, the cells nuclei were counter-stained with 4',6-diamidino-2-phenylindole (Sigma-Aldrich, MO, USA). The stained cells were then observed with a Leica TCS-SP5 confocal microscope (Leica Microsystems, Wetzlar, Germany).

FE simulation and the load and boundary constrains

We herein designed two FE simulation tests. The first FE simulation test was designed to observe the stress transmission of the structure. The bottom of cylinder base was immobilized, and a vertical force (100 N) was applied on the top of the porous scaffold and the solid scaffold. The surfaces between the base and porous scaffold/solid scaffold were defined as a kinematic constrain and allowed the plate to uniquely move in the vertical direction.

The second FE simulation test was designed to analyze the stress of the scaffold and surrounding bone tissue after implantation. The bottom of the bone was immobilized, and a vertical force was applied on the top of the bone. As the weight of an adult rabbit is within 3–5 kg, the applied force was set to 50 N. The surfaces between scaffold and bone was defined as the first FE simulation test.

Furthermore, the elastic modulus of the porous structure was simulated by Abaqus/Explicit FE code (SIMULIA, Rhode Island, USA) with a compression speed of 0.5 mm/min under the load of 100 kN.

FE model operation

The geometry of Ti6Al4V porous scaffold and assembly unit used in the first FE simulation test were made by Materialise Magics 19.0 software (Materialise, Leuven, Belgium). The geometry of bone used in the second FE simulation test was reconstructed by MIMICS 19.0 software (Materialise, Leuven, Belgium) using the data of a rabbit femur, and the hole was used to assemble the scaffold that was obtained by a Boolean Operator in Magics software. All the data were exported as STL files, and the meshing was operated by Materialise 3-matic 11.0 software (Materialise, Leuven, Belgium). The finished models were imported and assembled in the Abaqus 2017 (SIMULIA, Rhode Island, USA). The porous scaffold and the solid scaffold were consumed as Ti6Al4V, and the cylinder base was consumed as bone material. All the materials were considered isotropic and liner-elastic. The material parameters were selected form the literature, as shown in *Table 1* (45,46).

In vivo test

3D printing and scaffolds preparation

The scaffolds used in the *in vivo* test were 6 mm height with diameter of 5 mm, and the 3D entities were fabricated by a SLM 3D printing machine (EOSINT M280, EOS Ltd., Munich, Germany). The laser power in SLM process was 180 W and the layer thickness was 0.03 mm. The surface topography of the 3D printing scaffolds was observed by SEM. According to the standard [ISO 13314:2011 (47)] for compression of porous and cellular metals, the compression modulus of the scaffold was tested using an electronic universal testing machine (CMT5105; MTS System Corp., MN, USA) equipped with a 100 kN load cell, and a compression speed of 0.5 mm/min. The porosity of the scaffolds was calculated by using the formula: $P=(V_0-V)/V_0\times100\%$. Here, V_0 represents the apparent volume of the solid Ti6Al4V cylinder and V represents the absolute volume of the porous scaffolds. All the numerical values of the volume were obtained in the Magics 19.0 software.

The scaffolds were ultrasonically cleaned three times in acetone, ethanol, and dH_2O before use. For the PDA coating, the scaffolds were operated as same as the substrate preparation part. For the control group, the scaffolds were just cleaned by acetone, ethanol, and ultrasonically rinsed with dH_2O three times, and then dried with nitrogen gas.

Experimental animals and operation procedure

A total of 6 male New Zealand rabbits with the weight of 3 kg were enrolled into the experiment. All the rabbits were kept in a 12:12 h light-dark cycle in the animal house

of Drum Tower Hospital affiliated to Medical School of Nanjing University, and all surgical procedures were performed under anesthesia of lidocaine and propofol. All the PDA coating scaffolds were implanted into the right femur condyle, and the control scaffolds were implanted into the left femur condyle. The cefuroxime sodium was intramuscularly injected for 3 d after operation to avoid infection, and the calcein was intramuscularly injected at the 4th week after operation. All the rabbits were sacrificed at the 5th week after operation to measure the effect of early bone formation.

Micro computed tomography (CT) analysis and 3D reconstruction

The femurs were scanned in a VivaCT-80 micro-CT system (Scanco Medical, Brüttisellen, Switzerland) at 70 kV, 145 μA, field of view (FOV) of 63.9 mm, and a nominal isotropic image voxel size of 62.4 μm. The obtained images were converted to DICOM files for the following analysis. The bone volume/total volume was measured in the software of micro-CT system. The 3D reconstruction of scaffold and new bone was operated by MIMICS 19.0 software. To avoid the impact of metal artifact, we used a high voltage and the same threshold value to segment the titanium and bone tissue.

Histological analysis

After performing Micro CT analysis, the harvested femurs were fixed in formalin at 4 ℃ overnight, then rinsed with distilled water, dehydrated through graded alcohols, and embedded in polymethyl methacrylate (PMMA) without decalcification. Thin sections of 30 μm thickness were cut using a diamond-coated saw (310 CP; EXAKT, Germany). The sections were stained with Goldner trichrome staining, and the green fluorescence were observed using a fluorescence microscope (Olympus Corp., Tokyo, Japan). The bone bridging was determined in these sections as previously described (22,48). Briefly, the areas with bone tissues and scaffolds were projected onto the X-axis, and the stretches where bone formation had occurred were summed up on this plane. The numerical value was given in percentage of the defect width (5 mm).

Statistical analysis

The statistical analysis and exponential curve fitting were performed using SPSS 19.0 software (SPSS Inc., IL, USA) and IGOR Pro 6.12 software (WaveMetrics Inc., OR, USA). Data were presented as mean ± standard deviation (SD) and evaluated by an unpaired Student's *t*-test. $P<0.05$ was statistically considered

Results

Surface topography and EDS

The surface topography of Ti6Al4V film without and with PDA coating were shown in *Figure 1A*,*B*. The EDS results of the two groups were shown in *Figure 1C*,*D*. The composing elements of a composite surface element are shown in *Table 2*. The adhesion of PDA coating was observed by SEM, and an increase in the content of carbon and oxygen demonstrated the existence of PDA as well.

Cell adhesion and cell viability

The CCK-8 result was shown in *Figure 2A*, the cell viability on PDA coating films was higher than the uncoated films at 1 day of culture and stayed equal with control group after 14 days. The cell morphology after seeding for 4 h was observed by SEM and the results are shown in *Figure 2B*,*C*, the PDA could stimulate cell adherence after 4 h. The cell attachment on blank titanium plane and PDA coating groups in Day 1 (*Figure 2D*,*E*), Day 7 (*Figure 2F*,*G*), and Day 15 (*Figure 2H*,*I*) was demonstrated. All the cells were attached to the Ti6Al4V substrate in different time points, which implied that the concentration of dopamine and the reaction time were appropriate. The immunofluorescence staining has shown that the cell viability can maintain a high-level after 15 d of culture.

FE simulation and 3D printing

The color changed from red to dark blue that represented the stress variation from large to small on the stress nephogram. The results of *Figure 3A*,*B* showed that the color around the scaffold was clearly different. The area of sky blue around the solid scaffold was 2.358 mm^2, and the value increased to 5.792 mm^2 after the scaffold was changed to porous structure. In addition, small area of cyan could be observed at the bottom around the porous structure. The same phenomenon was found in *Figure 3C*,*D*, and the area surround the porous scaffold was green and red, which implied that the stress was ranged from 0.8137 to 4.445 MPa according to the legend. The average stress applied on the bone tissue around the implant was 1.28 MPa,

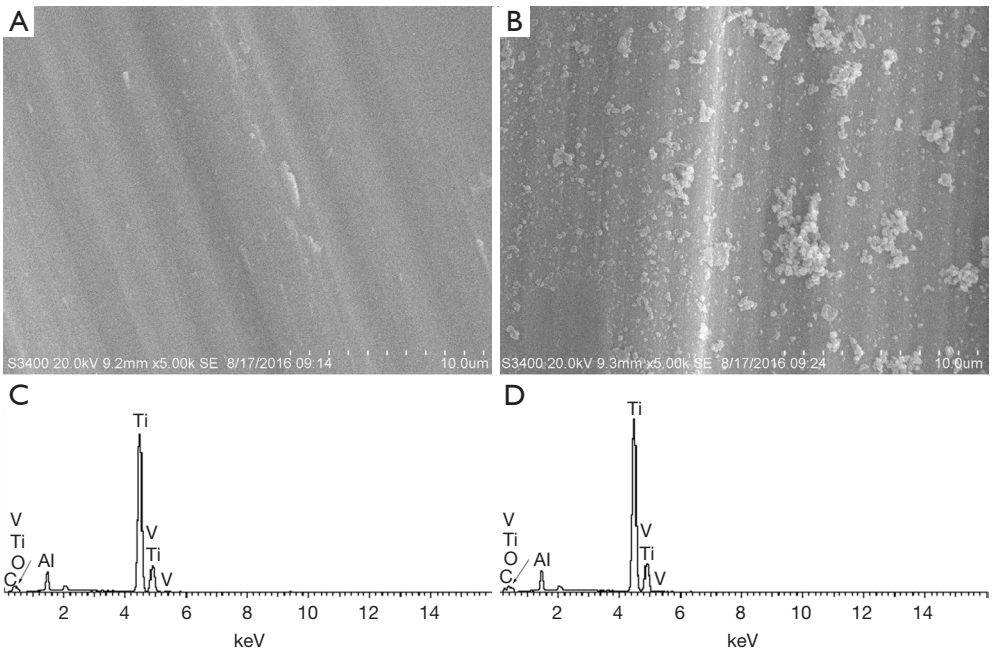

Figure 1 The results of SEM and EDS. (A) The SEM image of Ti6Al4V film without PDA coating; (B) the SEM image of Ti6Al4V film with PDA coating; (C) the EDS spectra of blank Ti6Al4V film; (D) the EDS spectra of Ti6Al4V film with PDA coating. PDA, polydopamine; SEM, scanning electron microscope; EDS, energy dispersive spectrometer.

Table 2 The surface element content

Element	Weight ratio % (with PDA)	Weight ratio % (without PDA)
Carbon	5.46	2.06
Oxygen	9.73	5.75
Aluminum	4.63	5.08
Titanium	77.00	83.48
Vanadium	3.18	3.64

PDA, polydopamine.

and the average stress on scaffold was 1.102 MPa.

The compression modulus of the scaffold analyzed by FE simulation and tested by an electronic universal testing machine is shown in *Figure 3E*. The scaffold commenced to yield at 258.98 MPa, and the elastic modulus was 11.2 GPa, which was close to the elastic modulus of cortical bone.

The structure and the general view of scaffolds were shown in *Figure 3F,G*. The pore size of the scaffolds was approximately 400 μm, that would be close to the structural design (*Figure 3H,I*).

Early osteogenesis evaluation

All rabbits recovered well from anesthesia and the operative procedure. No implant dislocation and incision infection occurred during the experiment. Bone formation was observed in both groups after 5 weeks of implantation from the result of 3D reconstruction, and the volume was significantly different between them (*Figure 4A,B*). The volume of regenerative bone tissue in PDA coating group was 9.559±0.286 mm^3, and the rate of bone value/total value (BV/TV) was 17.70. In control group, the corresponding values were 7.187±1.577 mm^3 and 13.66, respectively, which were obviously lower than PDA coating group (*Figure 4C*). The results of bone bridging were shown in *Figure 4D*, the newly formed bone bridged the defect to 85.57%±4.274% in the PDA coating group, and to 51.25%±4.703% in the control group.

Sections used for histological analysis are shown in *Figure 5A*. The Goldner trichrome staining and the fluorescence microscopy proved this result as well (The green fluorescence represented the newly formed bone tissue in the fluorescence images). In PDA coating group, the scaffold was surrounded by the blue-green, and green

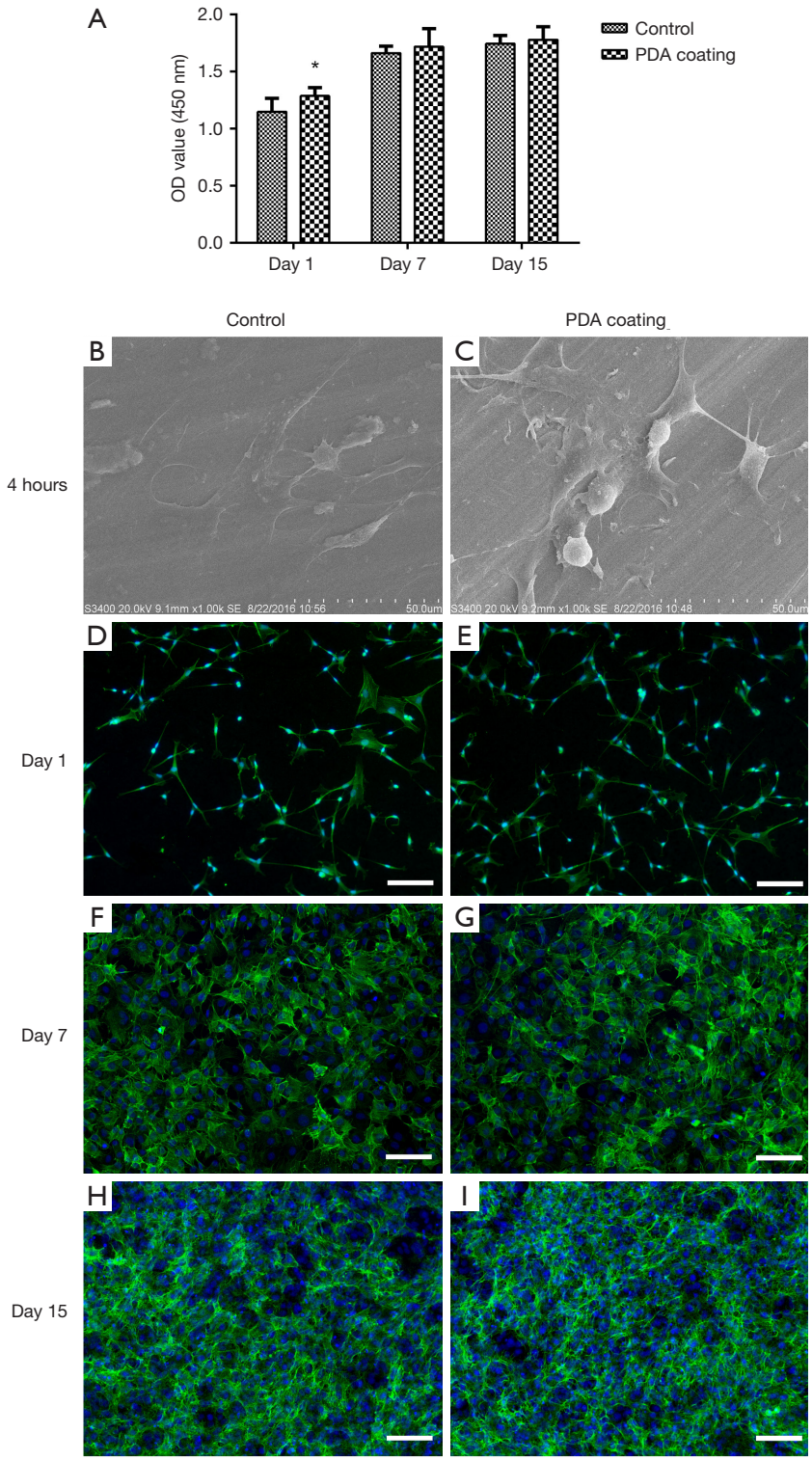

Figure 2 The results of cell behavior. (A) The CCK-8 results after 1, 7, and 15 d; (B,C) SEM micrographs showing MC3T3-E1 cell morphology cultured on unmodified Ti films and PDA coating films after 4 h of adhesion; (D,E) immunofluorescence staining showing cell morphology cultured on unmodified Ti films and PDA coating films after 1 d of adhesion; (F,G) 7 d of adhesion, and (H,I) 15 d of adhesion. Scale bar: 100 μm. PDA, polydopamine; SEM, scanning electron microscope.

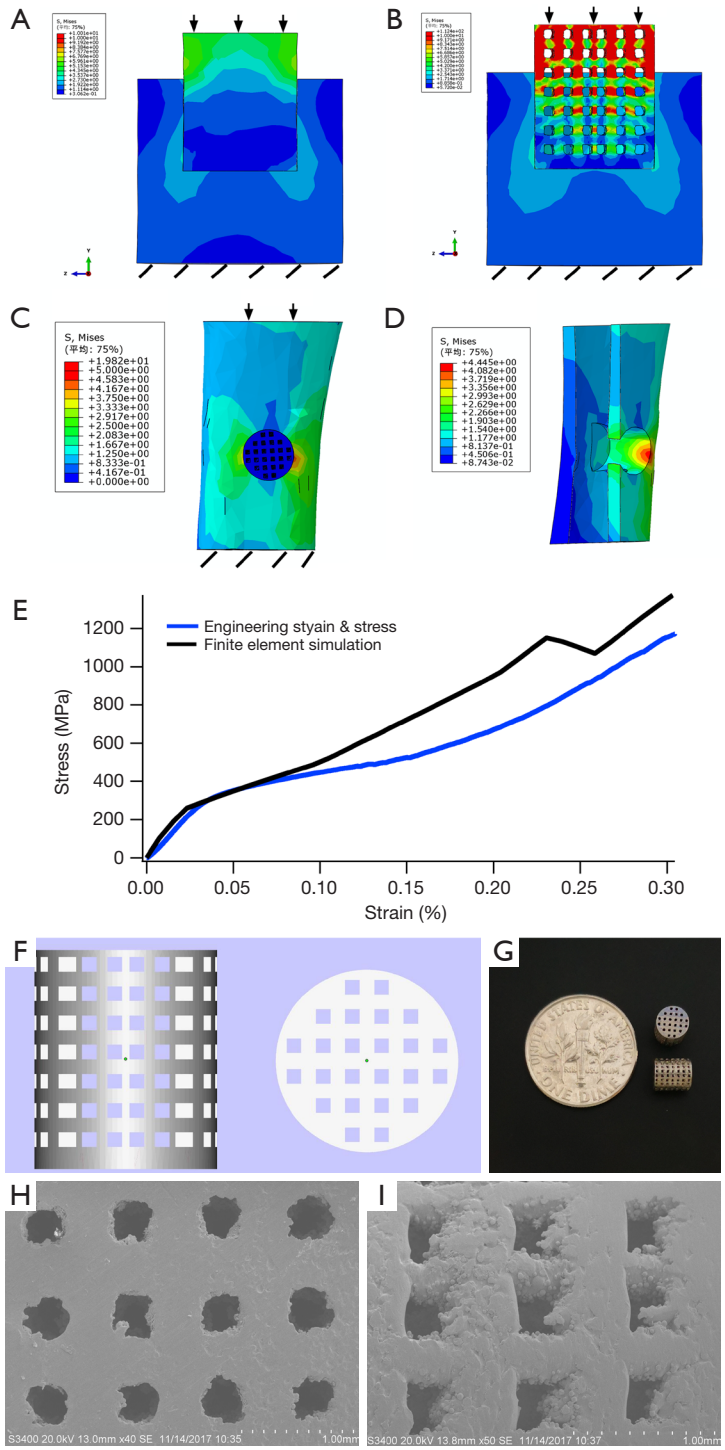

Figure 3 The results of FE simulation and 3D printing entities. (A) The stress transmission on solid scaffold; (B) the stress transmission on porous scaffold; (C) the general view of stress distribution after implantation with porous scaffold; (D) the internal view of stress distribution around the scaffold; (E) the arrow represented the direction of the force, and the oblique line represented the immobilization place; (F) the compression modulus of the porous scaffold, the black line represented the FE simulation result, and the blue line showed the compression test result; (G) the lateral and top views of the porous structure; (H) the general view of the 3D printing scaffolds, The SEM micrographs of the top view and (I) the lateral view of the scaffold. FE, finite element; SEM, scanning electron microscope.

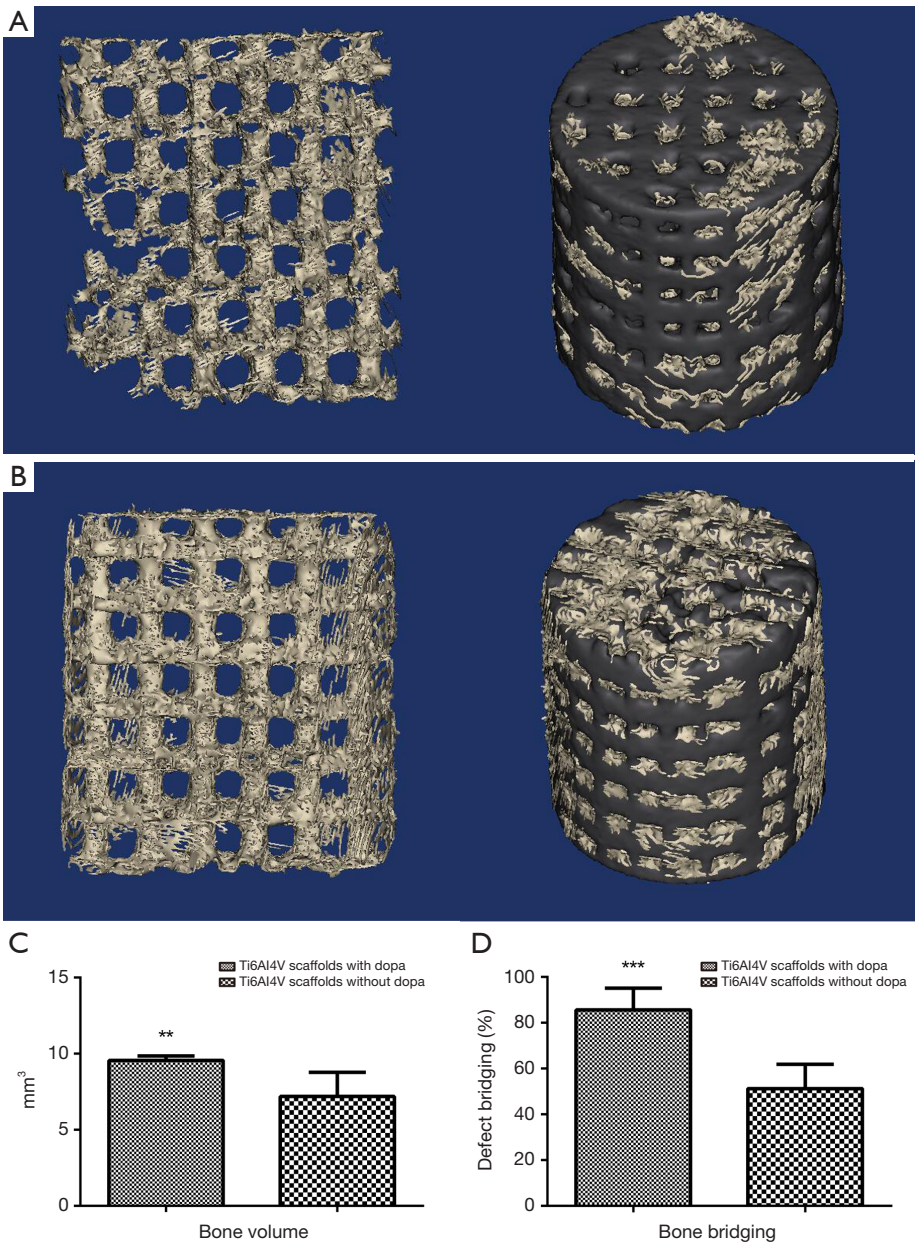

Figure 4 The results of new-born bone tissue evaluation. The 3D reconstruction of control group (A) and PDA coating group (B), the black part represented the scaffold and the silver part represented the newly formed bone tissue. The bone volume/total volume in two groups (C), the bone bridging in two groups (D). Data were shown as mean ± SD, with **, P<0.01; ***, P<0.001. PDA, polydopamine.

fluorescence was observed in the pores of scaffold in both sections, which indicated the bone growth inside the scaffold (*Figure 5B,C,D,E*). In control group, the blue-green and green fluorescence could be observed as well, however, the distribution area was significantly smaller than PDA coating group (*Figure 5F,G,H,I*).

Discussion

The results of the present study demonstrated that the osseointegration ability of porous Ti6Al4V scaffolds fabricated by SLM was improved by PDA with coating. This method of operation was simple and appropriate for early osteogenesis of titanium implants. A one-step

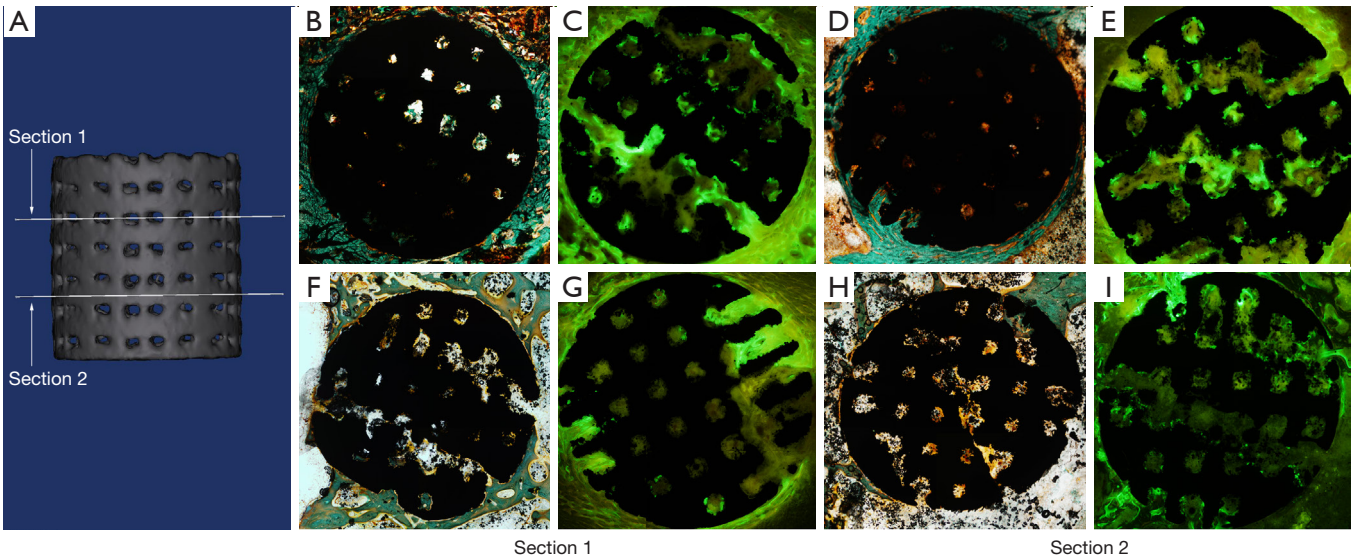

Figure 5 The results of histological analysis. The position of selected sections (A), the Goldner trichrome staining (B) and the green fluorescence (C) of PDA coating group in section 1, the Goldner trichrome staining (D) and the green fluorescence (E) of PDA coating group in section 2, the Goldner trichrome staining (F) and the green fluorescence (G) of control group in section 1, Goldner trichrome staining (H) and the green fluorescence (I) of control group in section 2. In Goldner trichrome staining, the color of blue-green represents the regenerating bony tissue. The green fluorescence represented the newly formed bone tissue in the fluorescence images. PDA, polydopamine.

reaction not only can modify the surface properties of titanium alloys, but also provide a stable layer to covalent immobilization with drugs and proteins (39). The mechanical reinforcement of PDA can be induced by the covalent crosslinking with amines and/or catechol or metal coordination, and the cell adhesion can be improved due to an increase in immobilization of serum adhesive proteins (30,49,50). The initial adhesion of MC3T3-E1 cell on the titanium surface was significantly enhanced from a short-time physical adsorption. The duration of reaction in several studies were ranged from 4 to 24 h, although we considered 40 min as an appropriate time-period (51-53). According to the previous research, only few minutes of dopamine deposition was sufficient to enhance cell adhesion, the lengthy reaction time had slight effect on cell attachment, which was consistent with Tsai *et al.*'s study (49). This phenomenon is formed because the thickness of PDA layer is a function of incubation time, increasing over the time (36). The thickness of the PDA layer can reach 50 nm after 24 h of reaction, and the substrate may be completely covered with PDA layer (49). It can be seen that the substrate film was partially coated by the PDA layer after incubation for 40 min. The difference between the coating and exposure of the film may lead to the difference in cell differentiation. In order to facilitate the observation of the effect of PDA coating on cell behavior, the Ti6Al4V substrate was selected to complete the cell viability test. Although the reaction time was short and the amount of PDA molecules were decreased, the mechanical stability of the coating layer was strong enough for the implantation applications. Previous studies have proved that the PDA coating can maintain its adhesion properties under strong ultra-sonication and other conditions, and the catechol—Ti adhesion force was four times stronger than biotin—streptavidin interactions (54-56). Additionally, the degradation time of PDA layers was relevant to the thickness of the layers in the physiological environment, the amount of carboxylic acid and amino functions can be maintained for more than 28 days according to the previous research (57). Thus, shortening the duration of reaction in dopamine solution is essential to minimize the thickness of PDA layer, but without effecting the cell adhesion ability, that would be crucial for the better application of this universal surface modification technology.

The SEM images, 3D reconstruction of micro CT analysis, and the serial sections demonstrated that the pore

size and the interconnectivity have been well controlled by SLM. The pore size can be maintained as 400 μm, which has been proved as the suitable size for bone formation (24). These properties are conductive to nutrients and oxygen exchange in the process of cell metabolism. In addition, the space in porous structure plays a momentous role in bone ingrowth and vascularization, which can lead to biological fixation at early stage of bone healing (11). The results of the *in vivo* study have confirmed this point of view. For some early implantation failure in dental and orthopedics, the implants with poor stability and lack of complete bone ingrowth are high risk factors (58,59). The histological evaluations demonstrated that new bone tissues were evenly distributed inside and around the scaffolds, and the PDA coating titanium scaffolds can acquire superior bone ingrowth in a short time-period. In the present study, we did not choose the long time points (e.g., 12 or 36 weeks), because the early osteogenesis is vital in achievement of mechanical stability at early stage. For rodents, duration of recovery within 2 months or longer is enough to fully heal the bone damage, and 4 to 5 weeks is effective and sufficient for observing the early bone formation (60-63).

Implants that are designed with a porous structure can decrease stiffness and avoid the stress shielding effect. The elastic modulus of a simple porous structure was herein calculated by FE simulation to match with the property of cortical bone that led to a superior stress transmission ability. Under applying of the equivalent force, we could observe that the stress on the porous scaffold was 10 times larger than that of solid scaffold. The stress on the porous structure gradually decreased from top to bottom, while the stress on the surrounding part gradually increased; therefore, the stress shielding effect was effectively decreased. In the second FE simulation test, we simulated the stress on the bone and the porous scaffold under the action of body weight. The peak stress on scaffold and bone tissue was 19.82 and 4.45 MPa, respectively. The average stress of scaffold and the surrounding bone tissue were both between 1 and 2 MPa. Based on Frost's research (10), 1 to 2 MPa is the threshold for bone regeneration, and the mentioned range will lead to gain in strength in the bone. The microscopic fatigue damage in bone is initiated if the stress increases to 20 MPa or above. The design of porous structure was simple, however, it can adequately match with the biomechanical requirements of regenerative bone in the experiment. However, the design process was far from real application. Evaluating the osteogenesis ability of the porous titanium scaffold using bionic design based on Voronoi Tessellation or triply periodic minimal surface (TPMS) is currently in progress (18,64).

Compared with synthetic bone scaffolds, the mechanical properties of porous titanium were more appropriate for providing sufficient initial mechanical support. By a one-step reaction with dopamine for short time-period, a proper biocompatible PDA layer can coat the surface of titanium, which not only can improve the early osteogenesis, but also provide the potential of immobilizing of other molecules to accelerate the bone healing process. The whole operation process can be carried out in few hours, providing an effective and novel treatment strategy. The dental implants, screws, artificial joints, and other titanium implants can be processed by PDA coating before or in the operation procedure.

There were still a number of limitations in this study. First, due to the lack of appropriate fixture, the push-out test was missed in the design of experiment, however, we have added this test in the osteogenesis evaluation of TPMS-based porous scaffolds. Second, we did not systemically analyze the specific relationship between the thickness of PDA layer, the immersion time, and the cell behavior, which is very significant for the results of surface modification. This issue may be included in our future research. Eventually, to minimize the potential factors and precisely explore the effect of PDA coating on porous titanium, we did not introduce BMP-2, growth factors, and drugs in the experiment. The combination of PDA coating with these components on scaffolds will be studied in the future as well.

Conclusions

In summary, we have demonstrated that the porous structure can be fabricated by SLM technology with parameters optimized in the present study. The pore characteristics can be precisely controlled as well. The FE simulation results indicated that biomechanical properties of the porous structure were appropriate for bone formation. Scaffolds can achieve superior bone integration under the coating of PDA. The bone ingrowth inside the PDA coating porous Ti6Al4V scaffolds was observed at the early stage of bone healing process. This simple and effective method can be helpful in the future clinical application of titanium implants.

Acknowledgments

Funding: This study was supported by the International Cooperation and Exchanges the National Natural Science Foundation (81420108021), Key Program of the National Natural Science Foundation (81730067), the National Natural Science Foundation (51575100, 51705259), the Special Program of Chinese Academy of Science (XDA16020805), Postgraduate Research & Practice Innovation Program of Jiangsu Province (SJKY19_0061) Jiangsu Provincial Key Medical Center Foundation and Jiangsu Provincial Medical Outstanding Talent Foundation.

Footnote

Conflicts of Interest: The authors have no conflicts of interest to declare.

Ethical Statement: All experimental protocols in this study were approved by the ethics committee of Drum Tower Hospital affiliated to Medical School of Nanjing University.

References

1. Meyrueis JP, Cazenave A. Consolidation des fractures. EMC - Rhumatologie-Orthopedie 2004;1:138-62.
2. Chien CY, Liu TY, Kuo WH, et al. Dopamine-assisted immobilization of hydroxyapatite nanoparticles and RGD peptides to improve the osteoconductivity of titanium. J Biomed Mater Res A 2013;101:740-7.
3. Khan SN, Tomin E, Lane JM. Clinical applications of bone graft substitutes. Orthop Clin North Am 2000;31:389-98.
4. Ryan GE, Pandit AS, Apatsidis DP. Porous titanium scaffolds fabricated using a rapid prototyping and powder metallurgy technique. Biomaterials 2008;29:3625-35.
5. Sidambe AT. Biocompatibility of Advanced Manufactured Titanium Implants-A Review. Materials 2014;7:8168.
6. Xu J, Weng XJ, Wang X, et al. Potential Use of Porous Titanium–Niobium Alloy in Orthopedic Implants: Preparation and Experimental Study of Its Biocompatibility In Vitro. PloS One 2013;8:e79289.
7. Li Z, Kawashita M. Current progress in inorganic artificial biomaterials. J Artif Organs 2011;14:163-70.
8. Parthasarathy J, Starly B, Raman S, et al. Mechanical evaluation of porous titanium (Ti6Al4V) structures with electron beam melting (EBM). J Mech Behav Biomed Mater 2010;3:249-59.
9. Chen Q, Thouas GA. Metallic implant biomaterials. Mater Sci Eng R Rep 2015;87:1-57.
10. Frost HM. A 2003 update of bone physiology and Wolff's Law for clinicians. Angle Orthod 2004;74:3-15.
11. Li G, Wang L, Pan W, et al. In vitro and in vivo study of additive manufactured porous Ti6Al4V scaffolds for repairing bone defects. Sci Rep 2016;6:34072.
12. Shi J, Yang J, Zhu L, et al. A porous scaffold design method for bone tissue engineering using triply periodic minimal surfaces. IEEE Access 2017;6:1015-22.
13. Boyan BD, Hummert TW, Dean DD, et al. Role of material surfaces in regulating bone and cartilage cell response. Biomaterials 1996;17:137-46.
14. Freyman TM, Yannas IV, Gibson LJ. Cellular materials as porous scaffolds for tissue engineering. Prog Mater Sci 2001;46:273-82.
15. Otsuki B, Takemoto M, Fujibayashi S, et al. Pore throat size and connectivity determine bone and tissue ingrowth into porous implants: three-dimensional micro-CT based structural analyses of porous bioactive titanium implants. Biomaterials 2006;27:5892-900.
16. Lopez-Heredia MA, Sohier J, Gaillard C, et al. Rapid prototyped porous titanium coated with calcium phosphate as a scaffold for bone tissue engineering. Biomaterials 2008;29:2608-15.
17. Loh QL, Choong CS. Three-dimensional scaffolds for tissue engineering applications : role of porosity and pore size. Tissue Eng Part B Rev 2013;19:485-502.
18. Shi J, Yang J, Li Z, et al. Design and fabrication of graduated porous Ti-based alloy implants for biomedical applications. J Alloys Compd 2017;728:1043-8.
19. Warnke PH, Douglas T, Wollny P, et al. Rapid prototyping: porous titanium alloy scaffolds produced by selective laser melting for bone tissue engineering. Tissue Eng Part C Methods 2009;15:115-24.
20. van der Stok J, Wang H, Amin Yavari S, et al. Enhanced bone regeneration of cortical segmental bone defects using porous titanium scaffolds incorporated with colloidal gelatin gels for time- and dose-controlled delivery of dual growth factors. Tissue Eng Part A 2013;19:2605-14.
21. van der Stok J, Lozano D, Chai YC, et al. Osteostatin-coated porous titanium can improve early bone regeneration of cortical bone defects in rats. Tissue Eng Part A 2015;21:1495-506.
22. de Wild M, Schumacher R, Mayer K, et al. Bone regeneration by the osteoconductivity of porous titanium implants manufactured by selective laser melting: a histological and micro computed tomography study in the

rabbit. Tissue Eng Part A 2013;19:2645-54.
23. Li Y, Zhou J, Pavanram P, et al. Additively manufactured biodegradable porous magnesium. Acta Biomater 2018;67:378-92.
24. Li K, Wang C, Yan J, et al. Evaluation of the osteogenesis and osseointegration of titanium alloys coated with graphene: an in vivo study. Sci Rep 2018;8:1843.
25. Jung HD, Yook SW, Han CM, et al. Highly aligned porous Ti scaffold coated with bone morphogenetic protein-loaded silica/chitosan hybrid for enhanced bone regeneration. J Biomed Mater Res B Appl Biomater 2014;102:913-21.
26. Diamanti MV, Del Curto B, Pedeferri M. Anodic oxidation of titanium: from technical aspects to biomedical applications. J Appl Biomater Biomech 2011;9:55-69.
27. Zhang W, Wang G, Liu Y, et al. The synergistic effect of hierarchical micro/nano-topography and bioactive ions for enhanced osseointegration. Biomaterials 2013;34:3184-95.
28. Wang G, Lu Z, Liu X, et al. Nanostructured glass-ceramic coatings for orthopaedic applications. J R Soc Interface 2011;8:1192-203.
29. Hu H, Zhang W, Qiao Y, et al. Antibacterial activity and increased bone marrow stem cell functions of Zn-incorporated TiO2 coatings on titanium. Acta Biomater 2012;8:904-15.
30. Chien CY, Tsai WB. Poly(dopamine)-assisted immobilization of Arg-Gly-Asp peptides, hydroxyapatite, and bone morphogenic protein-2 on titanium to improve the osteogenesis of bone marrow stem cells. Acs Appl Mater Interfaces 2013;5:6975-83.
31. Schuler M, Trentin D, Textor M, et al. Biomedical interfaces: titanium surface technology for implants and cell carriers. Nanomedicine (Lond) 2006;1:449-63.
32. Luginbuehl V, Meinel L, Merkle HP, et al. Localized delivery of growth factors for bone repair. Eur J Pharm Biopharm 2004;58:197-208.
33. Costa F, Carvalho IF, Montelaro RC, et al. Covalent immobilization of antimicrobial peptides (AMPs) onto biomaterial surfaces. Acta Biomater 2011;7:1431-40.
34. Shen CH, Cho YJ, Lin YC, et al. Surface modification of titanium substrate with a novel covalently-bound copolymer thin film for improving its platelet compatibility. J Mater Sci Mater Med 2015;26:79.
35. Michael J, Schönzart L, Israel I, et al. Oligonucleotide-RGD peptide conjugates for surface modification of titanium implants and improvement of osteoblast adhesion. Bioconjug Chem 2009;20:710-8.
36. Lee H, Dellatore SM, Miller WM, et al. Mussel-Inspired Surface Chemistry for Multifunctional Coatings. Science 2009;318:426-30.
37. Lee H, Rho J, Messersmith PB. Facile Conjugation of Biomolecules onto Surfaces via Mussel Adhesive Protein Inspired Coatings. Adv Mater 2009;21:431-4.
38. Choi YS, Kang H, Kim DG, et al. Mussel-inspired dopamine- and plant-based cardanol-containing polymer coatings for multifunctional filtration membranes. ACS Appl Mater Interfaces 2014;6:21297-307.
39. Wei Q, Achazi K, Liebe H, et al. Mussel-inspired dendritic polymers as universal multifunctional coatings. Angew Chem Int Ed Engl 2014;53:11650-5.
40. Lai M, Cai K, Zhao L, et al. Surface Functionalization of TiO2 Nanotubes with Bone Morphogenetic Protein 2 and Its Synergistic Effect on the Differentiation of Mesenchymal Stem Cells. Biomacromolecules 2011;12:1097-105.
41. Lynge ME, van der Westen R, Postma A, et al. Polydopamine--a nature-inspired polymer coating for biomedical science. Nanoscale 2011;3:4916-28.
42. Wu C, Han P, Liu X, et al. Mussel-inspired bioceramics with self-assembled Ca-P/polydopamine composite nanolayer: Preparation, formation mechanism, improved cellular bioactivity and osteogenic differentiation of bone marrow stromal cells. Acta Biomater 2014;10:428-38.
43. Xu M, Zhang Y, Zhai D, et al. Mussel-inspired bioactive ceramics with improved bioactivity, cell proliferation, differentiation and bone-related gene expression of MC3T3 cells. Biomater Sci 2013;1:933-41.
44. Lee JH, Lim YW, Kwon SY, et al. In vitro effects of mussel-inspired polydopamine coating on Ti6Al4V alloy. Tissue Eng Regen Med 2013;10:273-8.
45. Li L, Yang L, Yu F, et al. 3D printing individualized heel cup for improving the self-reported pain of plantar fasciitis. J Transl Med 2018;16:167.
46. Mircheski I, Gradišar M. 3D finite element analysis of porous Ti-based alloy prostheses. Comput Methods Biomech Biomed Engin 2016;19:1531-40.
47. Institution BS. Mechanical testing of metals. Ductility testing. Compression test for porous and cellular metals. Available online: https://infostore.saiglobal.com/en-au/Standards/Product-Details-271137_SAIG_BSI_BSI_625391/?ProductID=271137_SAIG_BSI_BSI_625391
48. Kruse A, Jung RE, Nicholls F, et al. Bone regeneration in the presence of a synthetic hydroxyapatite/silica oxide-based and a xenogenic hydroxyapatite-based bone substitute material. Clin Oral Implants Res 2011;22:506-11.

49. Tsai WB, Chen WT, Chien HW, et al. Poly(dopamine) coating of scaffolds for articular cartilage tissue engineering. Acta Biomater 2011;7:4187-94.
50. Guo L, Liu Q, Li G, et al. A mussel-inspired polydopamine coating as a versatile platform for the in situ synthesis of graphene-based nanocomposites. Nanoscale 2012;4:5864-7.
51. Kang J, Tada S, Kitajima T, et al. Immobilization of bone morphogenetic protein on DOPA- or dopamine-treated titanium surfaces to enhance osseointegration. Biomed Res Int 2013;2013:265980.
52. Yu X, Walsh J, Wei M. Covalent Immobilization of Collagen on Titanium through Polydopamine Coating to Improve Cellular Performances of MC3T3-E1 Cells. RSC Adv 2013;4:7185-92.
53. Cho HJ, Perikamana SK, Lee JH, et al. Effective immobilization of BMP-2 mediated by polydopamine coating on biodegradable nanofibers for enhanced in vivo bone formation. ACS Appl Mater Interfaces 2014;6:11225-35.
54. Ryu J, Ku SH, Lee H, et al. Mussel-Inspired Polydopamine Coating as a Universal Route to Hydroxyapatite Crystallization. Adv Funct Mater 2010;20:2132-9.
55. Lee H, Scherer NF, Messersmith PB. Single-Molecule Mechanics of Mussel Adhesion. Proc Natl Acad Sci U S A 2006;103:12999-3003.
56. Hong S, Lee JS, Ryu J, et al. Bio-inspired strategy for on-surface synthesis of silver nanoparticles for metal/organic hybrid nanomaterials and LDI-MS substrates. Nanotechnology 2011;22:494020.
57. Perez-Anes A, Gargouri M, Laure W, et al. Bioinspired Titanium Drug Eluting Platforms Based on a Poly-β-cyclodextrin-Chitosan Layer-by-Layer Self-Assembly Targeting Infections. Acs Appl Mater Interfaces 2015;7:12882-93.
58. Osman WS, Bassiony AA, Asal MK, et al. Failure of a properly positioned tantalum rod for treatment of early femoral head necrosis and conversion to total hip arthroplasty. Eur Orthop Traumatol 2015;6:409-15.
59. Chrcanovic BR, Albrektsson T, Wennerberg A. Reasons for failures of oral implants. J Oral Rehabil 2014;41:443-76.
60. Inzana JA, Olvera D, Fuller SM, et al. 3D Printing of Composite Calcium Phosphate and Collagen Scaffolds for Bone Regeneration. Biomaterials 2014;35:4026-34.
61. Amin Yavari S, van der Stok J, Chai YC, et al. Bone regeneration performance of surface-treated porous titanium. Biomaterials 2014;35:6172-81.
62. Wang F, Wang L, Feng Y, et al. Evaluation of an artificial vertebral body fabricated by a tantalum-coated porous titanium scaffold for lumbar vertebral defect repair in rabbits. Sci Rep 2018;8:8927.
63. Yu X, Wang L, Jiang X, et al. Biomimetic CaP coating incorporated with parathyroid hormone improves the osseointegration of titanium implant. J Mater Sci Mater Med 2012;23:2177-86.
64. Shi J, Zhu L, Li L, et al. A TPMS-based method for modeling porous scaffolds for bionic bone tissue engineering. Sci Rep 2018;8:7395.

Cite this article as: Li L, Li Y, Yang L, Yu F, Zhang K, Jin J, Shi J, Zhu L, Liang H, Wang X, Jiang Q. Polydopamine coating promotes early osteogenesis in 3D printing porous Ti6Al4V scaffolds. Ann Transl Med 2019;7(11):240. doi: 10.21037/atm.2019.04.79

